

Barbara KUCHARSKA

IDENTIFICATION OF SURFACE STRESS IN THE EXHAUST SYSTEM PIPE MADE BY HYDROFORMING TECHNOLOGY BASED ON DIFFRACTOMETRIC MEASUREMENTS

IDENTYFIKACJA NAPRĘŻEŃ POWIERZCHNIOWYCH W RURZE DO UKŁADU WYDECHOWEGO WYKONANEJ TECHNOLOGIĄ HYDROFORMOWANIA NA PODSTAWIE POMIARÓW DYFRAKTOMETRYCZNYCH*

In the work identification of surface stresses in the exhaust pipe made of Cr-Ni steel shaped with hydroforming technology. Stresses were determined by the non-destructive x-ray method $\sin^2\psi$. A complex state of tensile stresses with values in the range of 69÷240 MPa for circumferential stresses and 26÷290 MPa for longitudinal stresses was found on the surface of the pipe. The distribution of stresses on the circumference and length of the pipe was analyzed on the basis of coefficients of variation and wall thickness. A relationship was found between the value of surface stress and the wall thickness of the pipe. The highest stresses occurred in the areas of the pipe where the thickness of the wall was reduced the most. In the central part of the pipe, where the wall thickness reduction was the smallest, the stresses were also the smallest, but they were characterized by the highest dispersion of value. The distribution of surface stresses determined by diffractometric method was compared with the model of deformation of the pipe generated numerically.

Keywords: hydroforming, exhaust system, surface stresses, x-ray stress measurement.

W pracy dokonano identyfikacji naprężeń powierzchniowych w rurze wydechowej ze stali Cr-Ni kształtowanej technologią hydroformowania. Naprężenia wyznaczono nieniszczącą rentgenowską metodą $\sin^2\psi$. Na powierzchni rury stwierdzono złożony stan naprężeń rozciągających o wartościach z zakresu 69÷240 MPa dla naprężeń obwodowych i 26÷290 MPa dla naprężeń wzdłużnych. Rozłożenie naprężeń na obwodzie i długości rury analizowano na podstawie współczynników zmienności i grubości ścianki. Stwierdzono zależność pomiędzy wartością naprężeń powierzchniowych a grubością ścianki rury. Największe naprężenia występowały w obszarach rury gdzie grubość ścianki była najsilniej zredukowana. W centralnej części rury gdzie redukcja grubości ścianki była najmniejsza naprężenia również były najmniejsze, ale cechowały się największym rozproszeniem wartości. Rozłożenie naprężeń powierzchniowych wyznaczonych metodą dyfraktometryczną porównano z modelem odkształceń w rurze wygenerowanym numerycznie.

Słowa kluczowe: hydroformowanie, układ wydechowy, naprężenia powierzchniowe, rentgenowski pomiar naprężeń.

1. Introduction

For the production of exhaust systems in the automotive industry, ferritic steel sheets covered with aluminium alloy protective coatings are most often used presently. Aluminium coatings offer steel protection against the action of a corrosion medium at an elevated temperature, including combustion gas, and in the case of AlSi hot-dip coatings, also abrasion resistance [18, 19, 13]. Recently, it has been increasingly preferred to use austenitic steels in the production of exhaust systems [3, 4]. These steels have an extremely favourable combination of chemical properties and plastic forming capabilities [4, 6, 17]. The global production of these steels is still at a high level with a growing trend. 95% of the production of austenitic stainless steels are plastically shaped products, of which almost 10% are used in the automotive industry [6, 8]. The good plastic deformability of austenitic steels compensates for both their higher price, as well as the use of costly technologies, such as hydroforming.

Hydroforming is a method of forming flat metal sheets and closed sections using a fluid (most often water) under pressure (Fig. 1) [11, 1]. The advantage of the method in question is a reduction of the number of welded joints in structures and obtaining parts with a better

surface condition, thinner walls and better dimensional tolerance [14, 15, 5]. At present, forming sections by this method is most commonly used in the manufacture of bicycles (aluminium frames) and in the automotive industry. By hydroforming, car bodies, carrying frames, mufflers and other parts, including exhaust system components, are produced [9].

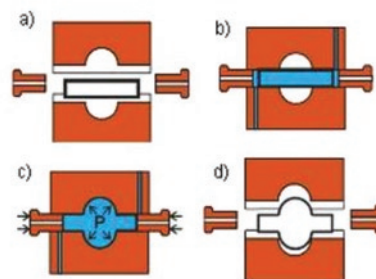


Fig. 1. Schematic diagram of the hydroforming operation: a – putting the pipe in the die, b – introducing a fluid inside the pipe, c – forming the pipe shape under fluid pressure, d – discharging the fluid and taking the formed part out of the die

(*) Tekst artykułu w polskiej wersji językowej dostępny w elektronicznym wydaniu kwartalnika na stronie www.ein.org.pl

By the hydroforming method it is possible to obtain complex shapes of parts with a varying curvature, which difficult to obtain by traditional plastic working method [3, 9, 10]. This is extremely important from the point of view of packing numerous items of car mechanics in the smallest space possible. At the same time, for closed sections, they must allow the free flow of media, such as combustion gas.

The specific conditions of hydromechanical forming of tubes, in which the material has no possibility of free “flowing” in the edge region, as is the case for sheets, cause high stresses to form in the material [7, 20]. The high stress level in a device’s part makes it susceptible to dimensional instability. What is more, even small mechanical or corrosion damage initiated during the operation of such a part will generate its disproportionately large deformation due to stress relaxation. Therefore, from the point of view of its service life it is essential to determine that stress by non-destructive methods and then to mitigate it. The present paper reports the results of stress measurements in an exhaust system pipe made by bending technology and hydroforming technology, respectively.

2. Material and testing methodology

The subject of research was a pipe designed for exhaust system, in which its final shape was imparted in the manufacturing process by hydroforming technology (Fig. 2). The pipe subjected to hydroforming had a wall thickness of max. 1.7 mm and was made of chromium-nickel steel in grade *X5CrNi18-10* (AISI 304L) with an austenitic microstructure (Fig. 3). The nickel concentration in the steel, as determined spectroscopically, was 9.6 wt%, which imparts a deep draw quality (DDQ) to the steel, compared to the standard version of grade 18-8.

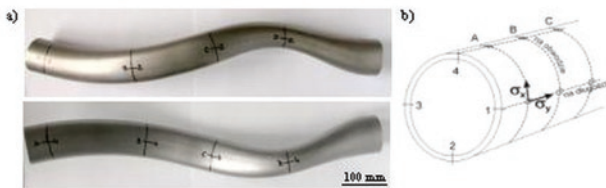


Fig. 2. a) A general view of the examined pipe and b) diagram of the location of the stress measurement places (σ) at outer surface of pipe. Sings: A, B, C and D – pipe perimeter, 1, 2, 3 and 4 – points on the pipe perimeter positioned every 90°

The objective of the research was to determine the stress on the outer surface of the pipe in the circumferential (x) and longitudinal (y) directions. For the purposes of testing, four regions (perimeters) were sectioned off on the pipe, of which three (denoted as B, C and D – Fig. 2a) were situated in the locations of a great change in pipe shape and one (denoted as A – Fig. 2a), near the pipe end, where the pipe cross-section was the closest in shape to circular. The stress magnitudes were determined at four points on the pipe perimeter (denoted as 1, 2, 3 and 4 – Fig. 2b), positioned every $\sim 90^\circ$ in such a manner that points, e.g. A1, B1, C1 and D1, be situated along one pipe generating line.

For determining the stress values, an X-ray diffraction method, referred to as the $\sin^2\psi$ method, was employed [16, 2]. Tests were performed based on the diffraction reflection from plane (311), which is preferably used in stress measurements in austenitic steels [12]. The measurements were taken using a PROTO diffractometer dedicated for stress measurements at the Materials Science Department, Faculty of Machines Construction and Aircraft Engineering, of the Rzeszow University of Technology (Fig. 4).

K_α Mn radiation (a $\varnothing 2$ mm collimator) of a wavelength of 0.2103 nm was used, which enabled stress to be measured in a sub-surface steel layer of a maximum thickness of 17 μm .

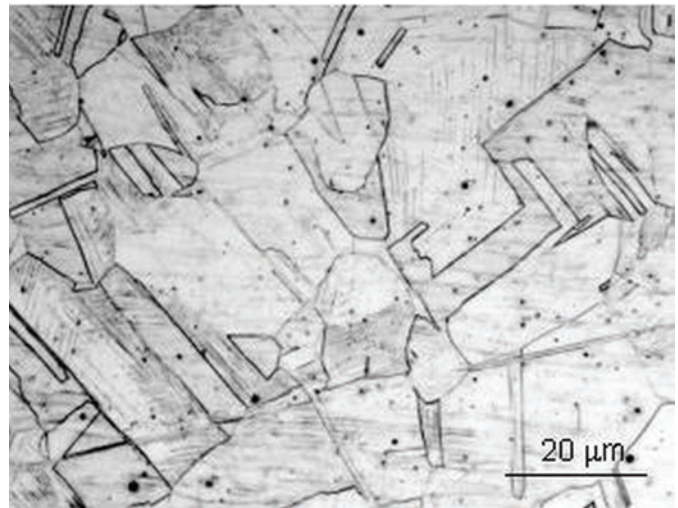


Fig. 3. Steel microstructure steel on the pipe cross-section

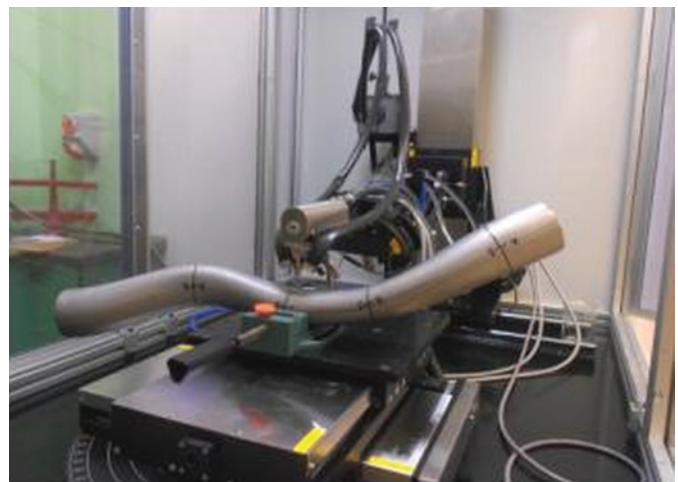


Fig. 4. The measurement of stress in the hydroformed pipe using a PROTO diffractometer

The stress determination by the X-ray method relies on the determination of crystal lattice deformation, ϵ , caused by, among other factors, by plastic working of polycrystalline material. This deformation is defined as the difference between interplanar distances Δd , in the material with stress and without stress. The stress, σ_ϕ , is calculated from relationship (1), where ϕ defines the stress direction (selected by positioning the part during measurement), while ψ - angle of diffractometer head positioning or part surface inclination in the measurement of d_{hkl} of the deformed lattice:

$$\epsilon_{\phi\psi} = \Delta d / d_o = \left(\frac{1+\nu}{E} \right) \sigma_\phi \sin^2 \psi + \left(\frac{\nu}{E} \right) (\sigma_{11} + \sigma_{22}) \quad (1)$$

where: d_o – distance between the lattice planes in the undeformed material ($d_o^{311}(\text{aust})=0.1083$ nm); σ_{11} and σ_{22} - principal stresses in the part surface (due to the measurement depth not exceeding a dozen or so μm , it is assumed that $\sigma_{33}=0$); ν - Poisson’s ratio; E – Young’s modulus [16].

The stress was calculated assuming the following X-ray elasticity constants for planes (311): $\frac{1}{2} s_2=6.33 \times 10^{-6} \text{ MPa}^{-1}$ and $-s_1=1.42 \times 10^{-6} \text{ MPa}^{-1}$ (the XRDWin software), whose values correspond to the mechanical constants of Young’s modulus of $E=200$ GPa and the Poisson ratio of $\nu=0.29$, according to relationship (2):

$$E = 1 / (s_1 + \frac{1}{2}s_2) \quad \text{and} \quad \nu = -s_1 / (s_1 + \frac{1}{2}s_2). \quad (2)$$

3. Results

The values of stresses determined by measurements on the pipe outer surface, as schematically shown in Figure 3b, are represented in Figures 5 and 6. All of the determined stresses were tensile stresses, both in the circumferential and longitudinal directions. The stress values were characterized by a large scatter, which was greater for longitudinal stress – the range of 21÷253 MPa, compared to the stress in the circumferential direction – the range of 65÷227 MPa.

The analysis of the stress distribution on the pipe perimeter (Fig. 5) showed that the greatest variation in stress magnitudes in both of the examined directions occurred on perimeter C in the central part of the pipe length. The most uniform stress distribution was found on perimeter D, whereas, circumferential stresses were, on average, greater than longitudinal stresses by approx. 80 MPa. The analysis of the stress distribution on the pipe length (Fig. 6) showed that the greatest diversity of circumferential stress magnitudes occurred on generating lines 4 and 3, while longitudinal stress magnitudes, on generating line 2. The most uniform distribution of circumferential stresses was found on generating lines 1 and 2, while longitudinal stresses, on generating line 3.

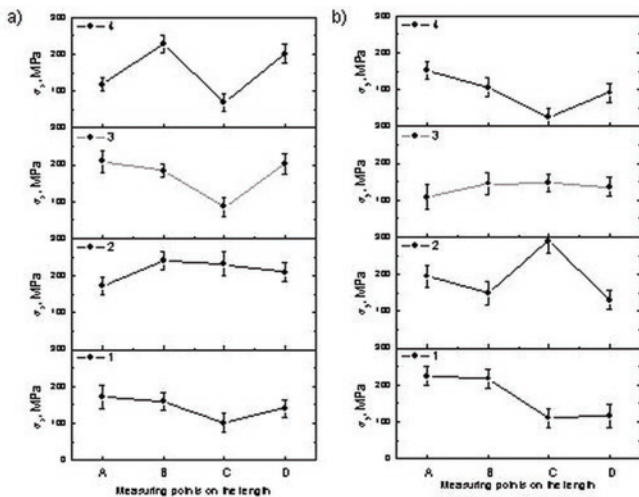


Fig. 5. The stress distribution on the pipe perimeter: a) circumferential stresses and b) longitudinal stresses

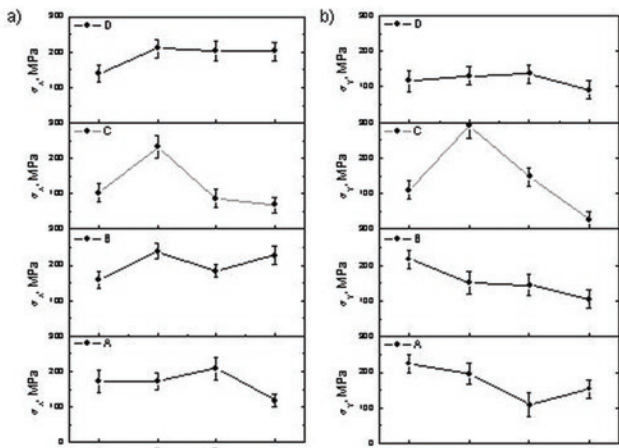


Fig. 6. The stress distribution on the pipe length a) circumferential stresses and b) longitudinal stresses

More generalized information on the distribution of residual stresses on the pipe surface can be provided by the averaged stress values for individual pipe regions (Fig. 7) and the coefficients of variation (Table 1) defined as (3):

$$V = S / \bar{\sigma} \quad (3)$$

where: S – standard deviation, $\bar{\sigma}$ - arithmetic average.

In the analysis of the average values of $\bar{\sigma}_x$ and $\bar{\sigma}_y$ stresses on respective pipe perimeters (A, B, C and D), no relationship between them was found (Fig. 7a). It can only be noted that the circumferential stress $\bar{\sigma}_x$ was the lowest one the central part of the pipe (on perimeter C). The average stress in the longitudinal direction, $\bar{\sigma}_y$ (Fig. 7a), was the highest in the vicinity of the pipe end represented by perimeter A, and decreased steadily towards perimeter D. It was also found that both circumferential stress and longitudinal, as determined in region C, exhibited the greatest coefficients of variation, V (61% and 77%), which means a large scatter of stress values in this pipe region. In turn, in region D, stresses in both directions showed the smallest coefficients of variation (17%), which means that a small scatter of stress values occurred there.

A similar trend in their distribution was found in the analysis of the average $\bar{\sigma}_x$ and $\bar{\sigma}_y$ stress values on individual pipe generating lines (1, 2, 3 and 4) (Fig. 7b). The highest average stresses characterized generating line 2, while the lowest, generating line 4. These generating lines lay on the opposite pipe walls. A large scatter of stress magnitudes in both directions occurred along generating line 4 (V=48% and 56%). A small scatter was shown by circumferential stress on generating line 2, and by longitudinal stress, on generating line 3.

Notwithstanding the similarity in circumferential and longitudinal stress distributions on the pipe generating lines, it should be underlined that the analysis of longitudinal stress distribution is not often seen as particularly useful for pipes. This is due to the fact under the pressure of a medium inside the operated pipe, it is primarily the circumferential stress that becomes augmented. Its magnitude on the outer surface is two times greater than that of longitudinal (axial) stress. For this reason, the risk of a pipe being damaged is associated chiefly with the magnitudes of circumferential stress – and it is this stress that both manufacturers and customers recommend to be determined. A pipe in a technological condition was investigated in this study. Under liquid pressure during hydroforming, no free widening of the pipe results due to the restriction of its shape by the die, so it can be presumed that the longitudinal stress may be relatively higher compared to circumferential stress. The stress values determined experimentally confirm this presumption with respect to the outer pipe surface.

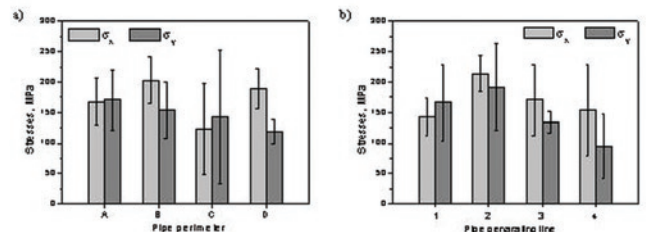


Fig. 7. The averaged stress values in respective regions of a hydroformed pipe: a) on the perimeters and b) on the generating lines (the error marks represent the standard deviation)

Due to the shape of the pipe and a small thickness of its wall it was not possible to take accurate hardness measurements directly on the

Table 1. The coefficients of variation, V , of stress in different hydroformed pipe regions

Circuit	$V(\sigma_x)$	$V(\sigma_y)$	Generating line	$V(\sigma_x)$	$V(\sigma_y)$
A	22	29	1	21	37
B	19	30	2	14	37
C	61	77	3	34	13
D	17	17	4	48	56

pipe surface, neither by the Vickers nor ultrasonic method. Nevertheless, the results of an attempt to take such measurements in approximation along generating line 1 are shown in Figure 8. The measurements were taken on the pipe surface between perimeters A, B, C and D in order not to damage the locations selected for stress measurements. Notwithstanding the only approximate character of the determined hardness values, it can be noticed that they reflected, to some extent, the distribution of σ_x and σ_y stresses along that generating line, i.e. they were smaller where stress values were also smaller. After stress measurements, sections were taken from the pipe to determine the wall thickness, which are also shown in Figure 8. The presumption that stresses are the highest in pipe regions with the smallest wall thickness, reduced during forming, was confirmed.

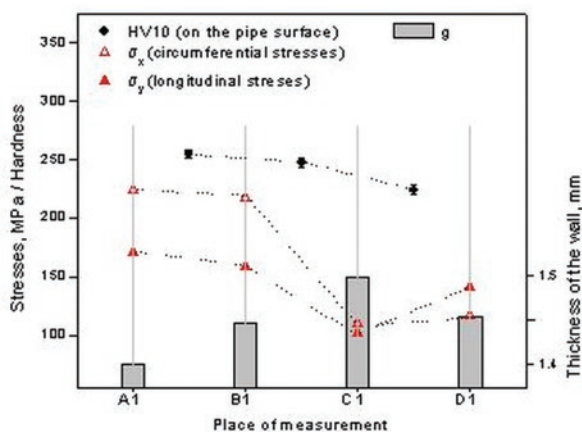


Fig. 8. Comparison of stress, hardness and wall thickness values on the pipe length (generating line 1)

4. Discussion and summary

A complex tensile stress state has been found on the outer surface of a chromium-nickel steel exhaust system pipe formed by hydroforming technology. The magnitudes of the highest surface stresses exceed the level of the yield point of steel 304L in version DDQ (approx. 170MPa). This means that the steel was strain hardened during hydroforming and, as can be presumed considering the complex shape of the pipe, also as a result of pre-bending preceding the hydroforming operation.

References

- Alaswad A, Benyounis K Y, Olabi A G. Tube hydroforming process: a reference guide. *Materials and Design* 2012; 33: 328-339, <https://doi.org/10.1016/j.matdes.2011.07.052>.
- Baczmański A, Wierzbowski K, Lipiński P. Determination of Residual Stresses in Plastically Deformed Polycrystalline Material. *Materials Science Forum* 1994; 157-162: 2051-2058, <https://doi.org/10.4028/www.scientific.net/MSF.157-162.2051>.
- Bahman K. Trends for stainless steel tube in automotive applications. *The Tube & Pipe Journal*, September 13, 2005 (thefabricator.com).
- Brytan Z. Stainless steel in the automotive industry (in Polish). *STAL Metale & Nowe Technologie* 2013; 11-12: 14-19.

The stresses were characterized by a wide range of variability both in the circumferential (σ_x) and the longitudinal (σ_y) directions, amounting to 69÷240 MPa and 26÷290 MPa, respectively. The analysis of the average values of stresses and variation coefficients found that the lowest stresses, having simultaneously the greatest scatter, occurred in the central part of the pipe, where the reduction of the wall thickness was the least. Considering the surface character of the determined stresses, the source of that scatter should be sought in differences in the conditions of friction against the die between different pipe surface fragments during hydroforming.

The distribution of surface stresses determined by the diffractometric method is generally consistent with the computer-generated model of strain distribution in individual pipe regions, shown in Figure 9. It should be emphasized, however, that at the wall thicknesses (<1.5 mm) possessed by the examined pipe, the model represents rather average strains within the whole wall thickness. It will not reflect any possible incidental phenomena (associated e.g. with transport and storage) which could occur in production conditions.

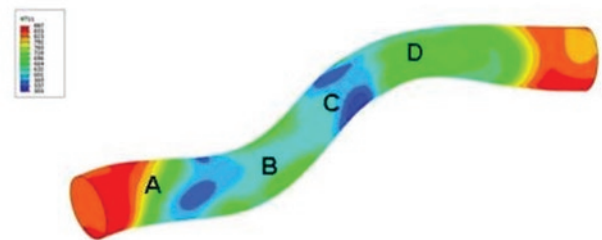


Fig. 9. The distribution of strains in the hydroformed pipe, generated from computer modelling

The values of determined stresses and the analysis of their distribution, based on measurements taken by the X-ray method, concern small surface areas defined by the cross-section of collimated radiation ($\varnothing 2\text{mm}$) and its penetration into the steel (approx. 17 μm) at the outer surface of the pipe. Depicting the distribution of stresses or strains within so thin layer is not achievable in computer modelling of plastic forming processes. Therefore, the X-ray method may only be used as a valuable complement to modelling, especially as modern diffractometers enable non-destructive measurements to be taken on thin-walled products of a complex surface shape.

Numerical analyses of the flow of a liquid medium in engine piping, presented in the literature, show that the medium exerts different pressure on the pipe walls in different pipe locations. This pressure depends primarily on the pipe bend angle and medium parameters, such as temperature, density or flow velocity [20]. This suggests that in locations, where the pipe curvature is the greatest, making stress distribution mapping by comprehensive measurements on the perimeters and along the pipe generating lines would be advisable.

5. Chałupczak J. Hydromechanical spreading in application to the formation of tees and X-pieces (in Polish). Works of the Kielce University of Technology. Mechanics; 39. Habilitation dissertation. Kielce, 1986.
6. Gronostajski Z, Kuziak R. Metallurgical, technological and functional foundations of advanced high-strength steels for the automotive industry (in Polish). Works of the Institute of Ferrous Metallurgy 2010; 22-26.
7. Hashemi R, Assemoir A, Masourni E, Abad K. Implementation of the forming limit stress diagram to obtain suitable load path in tube hydroforming considering M-K model. Materials & Design 2009; 30(9): 3545-3553, <https://doi.org/10.1016/j.matdes.2009.03.002>.
8. ISSF International Stainless Steels Forum. Stainless Steel Consumption Forecast, October 2017, (<http://www.worldstainless.org/statistics>) 05.12.2018
9. Kocańda A, Sadłowska H. Automotive component development by means of hydroforming. Archives of Civil and Mechanical Engineering 2008; 8(3): 55-69, [https://doi.org/10.1016/S1644-9665\(12\)60163-0](https://doi.org/10.1016/S1644-9665(12)60163-0).
10. Koç M. An overall review of tube hydroforming (THF) technology. Journal of Materials Processing Technology 2001; 108: 384-393, [https://doi.org/10.1016/S0924-0136\(00\)00830-X](https://doi.org/10.1016/S0924-0136(00)00830-X).
11. Koç M (Ed.). Hydroforming for Advanced Manufacturing. Woodhead Publishing Limited England, and CRC Press USA, 2008, <https://doi.org/10.1533/9781845694418>.
12. Kucharska B, Krzywiecki M. Stresses in a Cr-Ni superficial steel layer based on x-ray measurements and electropolishing Solid State Phenomena 2015; 223: 348-354, <https://doi.org/10.4028/www.scientific.net/SSP.223.355>.
13. Kucharska B, Wróbel A, Kulej E, Nitkiewicz Z. The X-ray measurement of the thermal expansibility of Al-Si alloy in the form of cast and a protective coating on steel. Solid State Phenomena 2010; 163: 286-290, <https://doi.org/10.4028/www.scientific.net/SSP.163.286>.
14. Miłek T. Variations of wall thickness in the sections of hydromechanically bulged copper cross joints. Eksploatacja i Niezawodność - Maintenance and Reliability 2003; 2(18): 45-48.
15. Morphy G. Pressure-sequence and high pressure hydroforming: Knowing the processes can mean boosting profits. The Tube & Pipe Journal, September/October 1998 (thefabricator.com, February 2001).
16. Skrzypek S J, Witkowska M, Kowalska M, Chruściel K. The non-destructive X-Ray methods in measuring of some material properties (in Polish). Hutnik-Wiadomości Hutnicze 2012; 79(4): 238-246.
17. Susceptibility of stainless steels to plastic working. Euro Inox, Series: Materials and applications. Book No. 8, 2008.
18. Wróbel-Knysak A, Kucharska B, The abrasion of Al-Si coatings with different silicon crystal morphology used in car exhaust systems. Tribologia 2016; 5: 209-218, <https://doi.org/10.5604/01.3001.0010.6701>.
19. Xianfeng Chen, Zhongqi Yu, Bo Hou, Shuhui Li, Zhongqin Lin. A theoretical and experimental study on forming limit diagram for a seamed tube hydroforming. Journal of Materials Processing Technology 2011; 211(12): 2012-2021, <https://doi.org/10.1016/j.jmatprotec.2011.06.023>.
20. Kumbár V, Votava J, Numerical modelling of pressure and velocity rates of flowing engine oils in real pipe. Eksploatacja i Niezawodność - Maintenance and Reliability 2015; 7(3): 422-426, <https://doi.org/10.17531/ein.2015.3.13>.

Barbara KUCHARSKA

Department of Production Engineering and Materials Technology
Czestochowa University of Technology
Armii Krajowej 19 str., 42-200 Czestochowa, Poland

E-mail: kucharska.barbara@wip.pcz.pl
